Elisar Barbar
Department of Chemistry and Biochemistry, Ohio University, Athens, OH 45701

NMR Characterization of Partially Folded and Unfolded Conformational Ensembles of Proteins

Abstract: *Studies of unfolded and partially folded proteins provide important insight into the initiation and process of protein folding. This review focuses on the use of nmr in characterization of ensembles of proteins that model the early stages of folding. Analysis of an ensemble includes description of the number of conformations, their structure, relative populations, interconversion rates, and dynamics of subconformations. A chemically synthesized analogue of bovine pancreatic trypsin inhibitor (BPTI), $[14–38]_{Abu}$, has provided a rare system for characterization of multiple partially folded conformations in slow exchange at near physiological conditions. Multidimensional nmr techniques coupled with selective labeling were used to probe different segments of the polypeptide chain. At each labeled site, there is evidence of slow interconversion between two families of partially folded conformations that in themselves are ensembles of rapidly interconverting conformers. All these conformers display significantly more order in the core relative to the rest of the molecule. For other variants of BPTI that are unfolded at equilibrium, the most ordered structure is also favored in the hydrophobic core residues of the native protein. This is consistent with the hypothesis that the residues that are the first to fold go on to form the most stable, structure-determining part of the protein.* © 1999 John Wiley & Sons, Inc. Biopoly 51: 191–207, 1999

Keywords: *unfolded and partially folded proteins; nmr; protein ensembles; bovine pancreatic trypsin inhibitor; $[14–38]_{Abu}$; selective labeling; hydrophobic core residues*

INTRODUCTION

Rapid folding to a specific compact structure is essential for the function of proteins. High-resolution structures of stable folded proteins and protein complexes from x-ray crystallography and nmr have lead to recent advances in understanding the mechanism of protein action, and are the basis for rational drug design strategies. Significant progress has concurrently been made in elucidating the process by which proteins acquire their folded structures. With the recognition that very large molecules possessing many degrees of freedom are unlikely to have a single, well-defined folding pathway, a new conceptual description for protein folding research has been developed.[1–6] This description emphasizes the existence of an ensemble of conformations at each stage of folding, and multiple transition states in a complex energy landscape. Recent developments in the theory of protein folding have been reviewed.[7–9] Here, we focus on direct nmr studies of conformational ensembles of partially folded and unfolded states. Structural characterization of these conformations provide insights into the nature of the ensemble at the *starting* point and *during* protein folding.

Since the work of Anfinson,[10] it has generally been accepted that the native state of proteins is at the

Correspondence to: Elisar Barbar; email: barbar@ohiou.edu
Contract grant sponsor: NIH
Contract grant number: GM 26242, GM 51628, and GM 17341
Biopolymers (Peptide Science), Vol. 51, 191–207 (1999)

CCC 0006-3525/99/030191-17

global minimum of the free energy surface for most proteins and that a landscape suitable for rapid folding is encoded into the amino acid sequence along with the structure of the native form. Thermodynamic stability and rapid folding have been selected in the evolution of native proteins. Identifying the forces in the protein that determine its ability to fold rapidly to a functional structure remains a considerable challenge. However, there is increasing demand for a reliable method for predicting the folded structure of the products of the gene sequences generated in the genome projects. An understanding of protein folding will no doubt aid in this effort.

Analysis of compact non-native states is leading to a more comprehensive understanding of naturally occurring misfolded proteins. There is accumulating evidence that diseases due to amyloidosis such as Kreutzfeld-Jakob disease, Alzheimer's disease and Parkinson's disease are caused by unfolded or misfolded proteins.[11–13] Formation of amyloid occurs when the native fold of a protein is destabilized while noncovalent interactions within the polypeptide chain remain favorable. Recent work suggests that a tendency to form amyloids is a general characteristic of partially folded proteins, and not just those associated with amyloid disease. For example, muscle acylphosphatase was found to produce amyloid fibrils when subjected for long periods to conditions known to favor the partially folded state.[14,15]

The lifetime of intermediate conformations in folding are too short for high-resolution structural studies, particularly for natural proteins at physiological conditions. To circumvent this problem, the protein or conditions must be modified, so that an ensemble of partially folded conformations can be studied at equilibrium. Partially folded proteins are considered models for transient species formed during kinetic refolding.[16,17] Their formation is commonly induced by extremes of solvent conditions such as low pH or addition of alcohol and other denaturants.[18–21] Partially folded proteins at equilibrium can also be formed by reduction of disulfide bonds, as for example, in bovine α-lactalbumin,[22] in bovine pancreatic ribonuclease A,[23] and in bovine pancreatic trypsin inhibitor (BPTI).[24–27] Specific point mutations or deletions of entire segments may also form partially folded proteins at equilibrium, as observed for staphylococcal nuclease.[28]

Studies of structured peptides corresponding to segments of a protein reveal intrinsic propensities of the polypeptide chain and may identify potential initiation sites.[29–31] Designed peptides are also useful as model systems for characterizing the interactions that stabilize secondary structure and for investigating protein structure and function.[32] Conformations of peptides can be stabilized by addition of trifluoroethanol, insertion of a disulfide bond at the terminal ends, or optimization of sequences for enhancement of stability.[33] In isolated peptide fragments of myoglobin, a strong correlation between the residual structure of the peptides and the ordered segments detectable during folding of the intact protein was observed. In BPTI peptides that show helical propensities, however, only one is helical in native BPTI while the other two are extended β-strands.[34] Helical propensities of peptide fragments are based either on residue prediction or on whether isolated peptides form helical conformations in trifluoroethanol. This example illustrates the difficulty in extrapolation from the structure of isolated peptides to the folded protein.

Multidimensional nmr studies of denatured proteins are the subject of several recent reviews.[35–37] Characterization of the structure and dynamics of multiple partially folded or unfolded conformations is limited by crowded spectra with severe line broadening. Examples include the molten globule form of α-lactalbumin, the denatured staphylococcal nuclease, and apomyoglobin. In α-lactalbumin, the absence of observable cross peaks under molten globule or partially folding conditions, along with the presence of sharp peaks under unfolding conditions, is explained by broadening due to intermediate exchange.[38] Similarly, in partially folded staphylococcal nuclease, some residues are in intermediate exchange and therefore apparently obscured by broadening; their cross peaks appear under unfolding conditions.[39] In apomyoglobin, two distinct partially folded states are detected under different solvent conditions.[40] Several other partially folded and denatured proteins sample conformations that are in fast or intermediate interconversion on the nmr time scale.[41–43]

The partially folded ensemble of a BPTI analogue shows equilibria that are more complicated: there is a *slow* exchange between a more ordered conformation, P_f, and a less ordered conformation, P_d.[26,44,45] Each conformation is itself an ensemble of rapidly interconverting conformers. Figure 1 is a diagram of native BPTI with three disulfide bonds, two in or close to the hydrophobic core (5–55, 30–51) and one in the flexible loops (14–38). To move the conformational distribution towards partially folded species, we retain the 14–38 cross-link in the flexible loops distant from the core.[27] A schematic diagram to illustrate this process is shown in Figure 2A and B. Cysteine residues 5, 55, 30, and 51 are replaced by α-aminobutyric acid (Abu). Abu is the same size (isosteric) as cysteine. The resultant protein favors a native-like core

while the rest of the molecule is more flexible.[26] To prepare fully unfolded variants, key tyrosine residues in the hydrophobic core of the single disulfide variant were replaced by alanine. A set of chemically synthesized variants allows characterization of native, partially folded, and unfolded BPTI at the same solvent and temperature conditions. The chemical synthesis used to access these molecules, including variants containing stable isotopically labeled residues, is described elsewhere.[46] Structures of the resultant BPTI analogues, which are either partially folded or completely unfolded, are characterized by two-dimensional ^{1}H homonuclear and ^{15}N heteronuclear nmr methods. Other single disulfide variants of BPTI connecting residues 5–55, or 30–51 where cysteine residues are replaced by either alanine or serine, have been characterized by nmr,[24,47–49] but full analysis of conformational exchange apparent in multiple peaks was not made.

Partially folded BPTI, with a single cross-link in the flexible loops, favors a relatively stable native-like core, while the rest of the molecule is more disordered and samples multiple conformations. The most stable part is not near the single cross-link but rather in the slow exchange core. Multiple conformations interconvert slowly on the nmr time scale, giving rise to separate sets of peaks. Each set corresponds to an average conformation of rapidly interconverting conformers. Figure 2C is a schematic representation of the partially folded ensemble showing multiple different conformations separated by different barriers. For unfolded BPTI ensemble, there are multiple conformations in fast and intermediate exchange. Even though there is no stable secondary or tertiary structure detected by CD, nmr spectra show significant differences in residual structure between the unfolded, fully reduced, and the unfolded variants with a single disulfide bond. The nmr characterization of multiple conformations of partially folded and unfolded BPTI gives a microscopic view of the incremental development of structure and of the changes in dynamics of different segments of the protein. The conformational diversity of unfolded and partially folded ensembles of BPTI suggests that folding occurs by multiple paths. At all stages of folding, native-like nonlocal interactions in the core are more stable than those in the rest of the molecule.

NMR PARAMETERS FOR DESCRIPTION OF ENSEMBLES

Analysis of nmr spectra of partially folded or unfolded proteins is complicated by extensive overlap in amide and aliphatic cross-peaks in the "random coil" region. The deviation of the observed chemical shifts from random coil values contains contributions from secondary and tertiary structural elements.[50] Figure 3 shows a comparison between native, partially folded, and unfolded BPTI ^{1}H-^{1}H nuclear Overhauser effect spectroscopy (NOESY) spectra. For the partially folded species (middle spectrum), downfield-shifted α-proton ($>$4.8 ppm), and amide signals (6.5–10.1 ppm) are diagnostic of some native-like conformers among the many conformers populated. In the unfolded spectrum (left), no peaks outside the random coil envelope are observed indicating the absence of stable secondary and tertiary structures.

Another parameter sensitive to the chemical environment is the nuclear Overhauser effect (NOE). For native proteins, the principle use of NOE in nmr analysis is interatomic distance determination. For partially folded and unfolded proteins, the intensity of NOE peaks is also affected by conformational exchange, and hence reflects both proximity and population. For example, a weak peak intensity may be assigned either to a long-range NOE or a short- to medium-range NOE of a less populated conformation. Moreover, in partially folded and unfolded proteins, there may be NOEs for a particular residue that are not consistent with one structure, suggesting that the residue is sampling different conformations. A single residue may have NOEs due to both extended structure and turn-like helical structure.

Slow chemical exchange on the nmr time scale is inferred from additional peaks in several types of spectra. Slow exchange arises when the same proton has a different chemical shift in each of two or more conformations that interconvert on the chemical shift time scale of ms or longer, thereby giving rise to a distinct signal for each conformation.[51] In rotating frame NOE spectroscopy (ROESY) spectra, the cross peaks due to chemical exchange are assigned to those having the same sign as the diagonal peaks, while cross peaks due to the NOE effect are of opposite sign.[52] In NOESY spectra, cross peaks due to chemical exchange are observed, in addition to cross peaks due to NOE, if the exchange rate is of the same order of magnitude as the NOESY mixing time. In total correlated spectroscopy (TOCSY) spectra, cross peaks in the amide–amide region are easily assigned to exchange cross peaks because no other correlations are generally observed in this region.

Resonance assignments for $[14–38]_{Abu}$ (BPTI with a single disulfide bond between residues 14 and 38 and the other cysteines are replaced by Abu) were obtained from homonuclear NOESY and TOCSY spectra. After assignments of all residues, there were

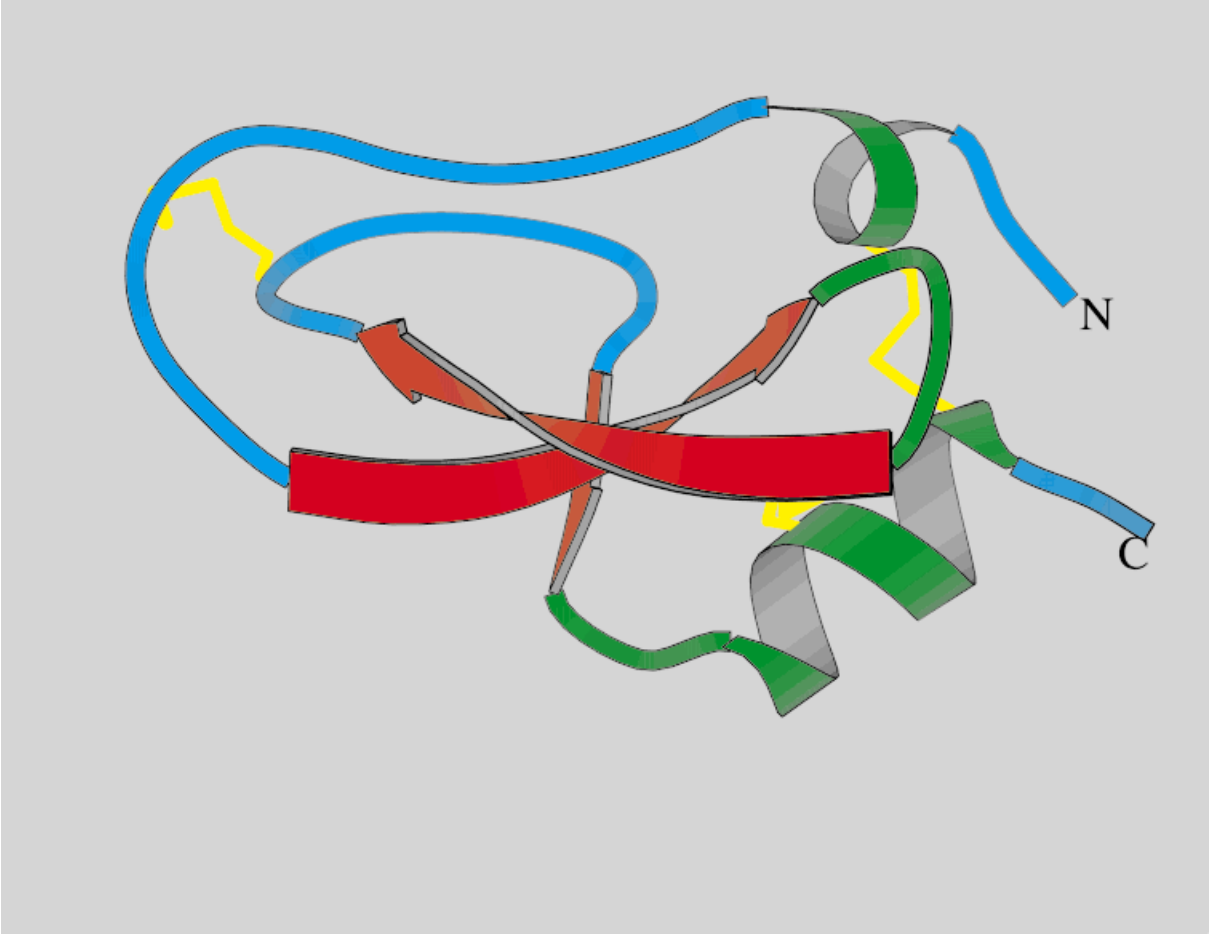

FIGURE 1

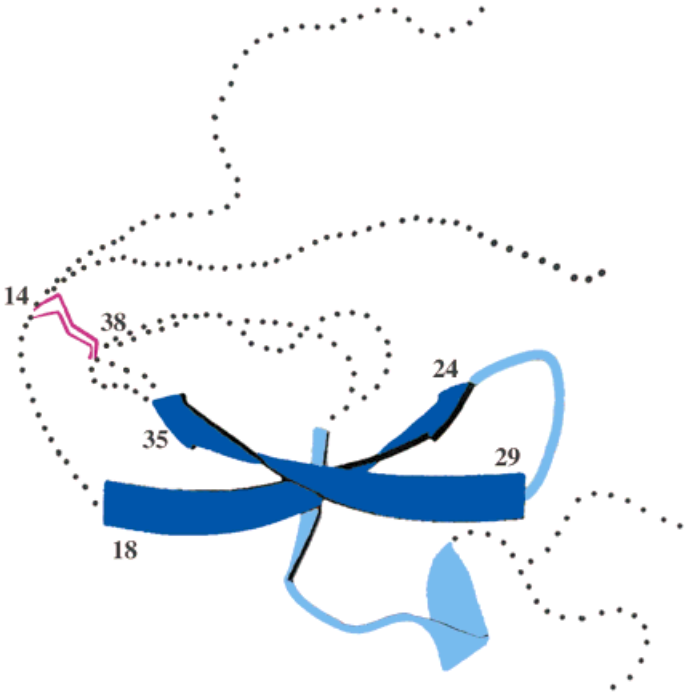

FIGURE 5

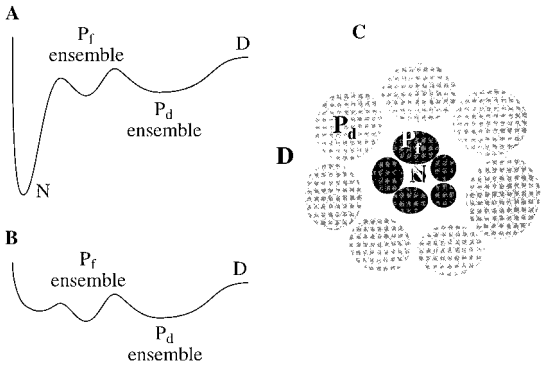

FIGURE 2 Representation of partially folded ensemble in a schematic energy diagram during folding. (A) Folding of native protein from a denatured state (D) to partially folded ensembles, P_f and P_d, that are transiently populated, then to native state (N), which is the lowest in energy. (B) Ensemble distribution in $[14–38]_{Abu}$; upon removal of two disulfide bonds, the P_f and P_d ensembles are the major conformations populated at equilibrium. P_d is more flexible and hence is sampling a wider distribution (broader minima). It is our working hypothesis that P_f and P_d in $[14–38]_{Abu}$ are representative of the same ensembles present in native BPTI. (C) A model of the distribution of partially folded conformations relative to native and denatured states based on $[14–38]_{Abu}$ data. The partially folded state PF consists of a more ordered family of conformers P_f (dark ovals) and a family of less ordered conformers P_d (light larger ovals). P_d conformers occupy a large conformational space, consistent with their observed flexibility. The size, number, and colors of circles reflect differences in entropy. The native conformation is represented in single, small, and dark circle. There is slow interconversion between conformers of P_f and conformers of P_d, illustrated by large barriers (white space between P_f and P_d circles). Within P_f and P_d conformers there are differences, illustrated in different shapes. Different conformers within P_f and P_d are also separated by barriers that are smaller in P_f (fast exchange) relative to P_d (intermediate exchange).

still additional unassigned peaks in or close to the random coil region. The additional peaks show correlations in TOCSY and NOESY spectra, indicating that they are "exchange" peaks of the same NH, and not a contaminant or peptide fragment. Furthermore, the purity of all nmr samples were verified by mass spectrometry, reverse phase C4 high performance liquid chromatography and gel electrophoresis. The additional peaks are assigned to a more disordered conformation, P_d, in slow exchange with a more ordered conformation, P_f. Cross peaks that correspond to the P_d conformation are assigned by their NH–NH correlation to the dispersed and more easily assigned peaks of P_f, and verified by identification of the respective spin systems in full TOCSY spectra. NH–NH correlations for several amide protons were observed in ROESY, NOESY, and TOCSY spectra.

To assign the overlapping peaks in the random coil region, we made use of peptide synthesis, to selectively label with ^{15}N several residues in different segments of the polypeptide chain. $^{15}N–^{1}H$ heteronuclear single quantum coherence (HSQC) spectra of the selectively labeled protein show two sets of peaks consistent with the presence of multiple conformations in slow exchange. Figure 4 shows $^{15}N–^{1}H$ HSQC with ^{15}N labels inserted at nine positions. The population of each NH in different conformations is obtained from peak intensities. Assignment of different peaks for the same NH was based on their correlation in $^{15}N–^{1}H$ exchange experiments. Spectra obtained at different mixing times show four peaks for every NH: one for each conformation P_f and P_d, and two other less intense peaks for exchange between P_f and P_d. The correlation peaks vary with the mixing time and allow for obtaining interconversion rate constants at equilibrium conditions.[45]

Peak line widths may also be informative in spectra of partially folded and unfolded states. The major contributors to line broadening are intrinsic relaxation rate constants as well as the presence of multiple interconverting conformations in the millisecond–microsecond intermediate exchange regime. Spectra of denatured species may show different peak intensities and line width broadening for different residues. A

FIGURE 1 Ribbon drawing of native BPTI. Colored in red is the central core of the protein, which includes residues that correspond to the slow exchange core. The three disulfide bonds 14–38, 30–51, and 5–55 are in yellow.

FIGURE 5 A model of the ensemble of the partially folded BPTI analogue $[14–38]_{Abu}$. The more ordered conformation, P_f, of the central antiparallel β-sheet between residues 18–35 favors a native-like conformation (blue). A small population of the residues is in a more disordered P_d conformation (not shown in this drawing but illustrated in Figure 6). The small β-bridge, β-turns, and first turn of the C-terminal helix have a less favored native-like P_f conformation (light blue). The rest of the molecule is disordered and samples two families of conformations P_f and P_d that are both non-native (two sets of dotted lines).

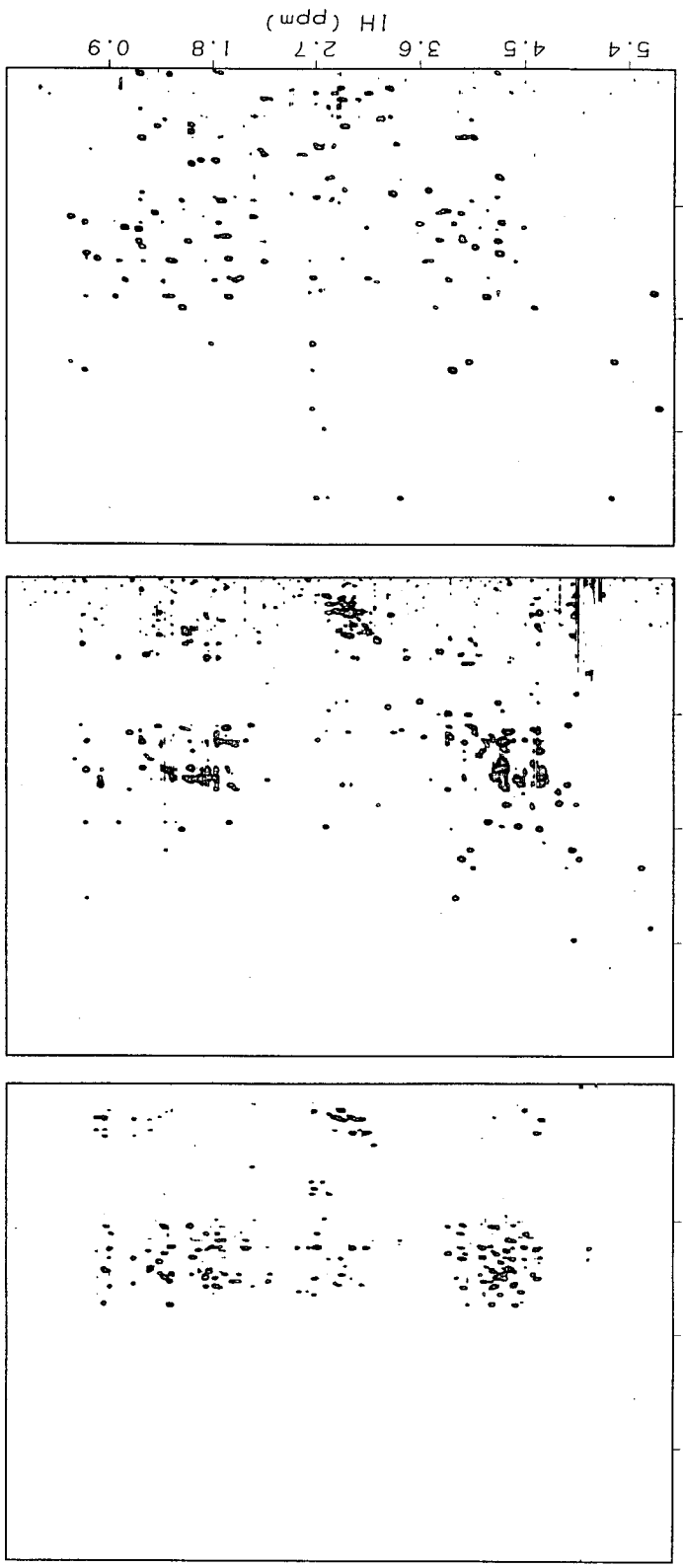

FIGURE 3 Comparison of peak dispersion in spectra of native (right), partially folded (center), and unfolded protein (left). ^{1}H–^{1}H NOESY spectra are shown, for example, at 5°C and pH 5.0, for native BPTI, partially folded $[14–38]_{Abu}$, and unfolded Y21A$[14–38]_{Abu}$.

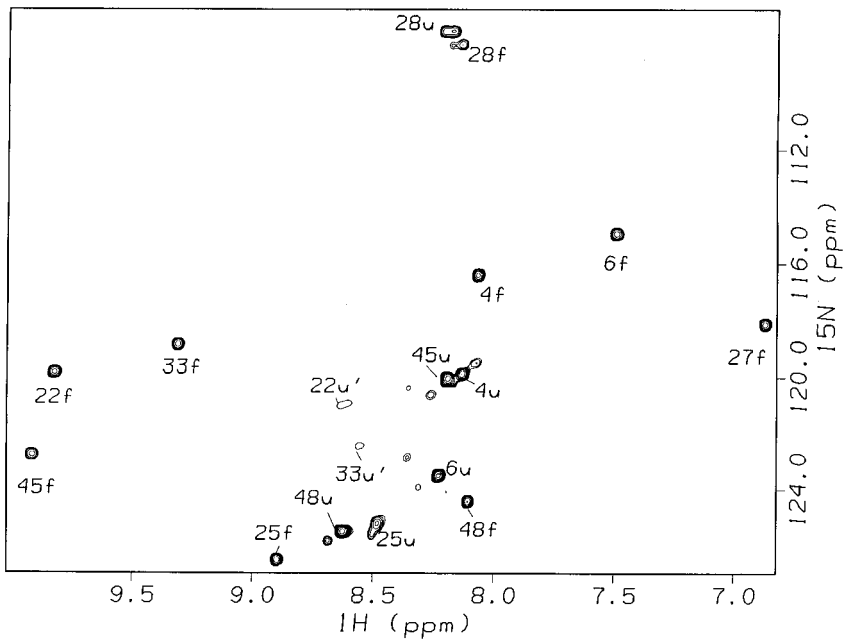

FIGURE 4 ^{1}H–^{15}N HSQC spectrum of $[14–38]_{Abu}$ with ^{15}N labels inserted at nine sites. The additional peaks (labeled u) are assigned to a less ordered conformation, P_d, in slow exchange with a more ordered conformation, P_f, represented by (f) peaks. A relaxation delay of 3 s was used; this is sufficiently longer than T_1 values to permit quantitative volume integration. The relative population of P_f and P_d are determined from peak intensities. Ala 27 (u) is too broad and hence not observed at the noise level plotted here. The spectrum was acquired at pH 5.0 and 5°C. At higher temperature, the intensities of the (f) peaks decrease while those of (u) peaks increase. The temperature dependence curve is shown in Figure 7 (right).

dramatic difference in peak broadening is observed for residues in the P_d conformation of the partially folded BPTI analogue. For example, in the HSQC spectrum of Figure 4, the line width of 22 (u) corresponding to the P_d conformation is 40 Hz, significantly broader than the line width of 6 (u) of 16 Hz. Differences in line broadening among residues imply that P_d samples many conformations with residues in the core, i.e., 22 and 33, being in a more ordered conformation than residues 4, 6, and 48.

A number of multidimensional, multinuclear nmr techniques are available to evaluate the conformational equilibria of proteins on faster time scales.[53,54] Table 1 summarizes the kind of information obtained from nmr experiments. The usefulness of these measurements in denatured proteins is in identifying the segments that are motionally restricted in the absence of stable secondary and tertiary structures. For motions on the picosecond–nanosecond time scale, relaxation parameters obtained from T_1 (longitudinal relaxation time constant), T_2 (transverse relaxation time constant), and NOE data give qualitative information about local flexibility. For example, local anisotropic motion in disordered segments of partially folded BPTI leads to longer T_1 and T_2, and negative or small positive NOEs.[53,54] To obtain spectral density functions $J(\omega)$, for both conformations P_f and P_d, standard equations reviewed in Daragan and Mayo[55] were used.

$$1/T_1 = (d^2/4)\,[J(\omega_H - \omega_N) + 3J(\omega_N) + 6J(\omega_H + \omega_N)] + k_{CSA}\,J(\omega_N)$$

$$1/T_2 = (d^2/8)\,[4J(0) + J(\omega_H - \omega_N) + 3J(\omega_N) + 6J(\omega_H) + 6J(\omega_H + \omega_N) + k_{CSA}/6)\,[3J(\omega_N) - J(0)] + R_{ex}$$

$$NOE = 1 + (d^2/4)\,(\gamma_H/\gamma_N)\,[6J(\omega_H + \omega_N) - J(\omega_H - \omega_N)]$$

where CSA is the chemical shift anisotropy that leads to an additional significant relaxation contribution, d is a proportionality constant, and γ_H, γ_N are the gyromagnetic ratios of H and N, respectively. The values of T_1, T_2, and NOE have the exchange contribution factored out as shown elsewhere.[45]

Since there are five frequencies and only three relaxation parameters measured, the values of spectral density functions may not be extracted without assumptions. In the model-free spectral density ap-

Table I Relaxation Parameters for Fast and Intermediate Motions

NMR Parameters	Information
Experimental parameters (T_1, T_2, NOE)	Local flexibility and internal mobility
Spectral densities ($J(0)$, $J(w_N)$, $J(w_H)$)	Global tumbling and internal mobility
Motional order parameters (S^2)	Restriction of internal motion
Overall correlation time (t_0)	Overall tumbling and compactness
Low T_2, high $J(0)$	Intermediate exchange

proach of Lipari and Szabo, the assumption is that the macromolecule tumbles isotropically in solution. This means that the correlation function describing the dynamics of the amide bond vector can be separated into fast internal motion (S^2 and τ_e), and slow overall molecular tumbling (τ_o). Order parameters S^2 are a measure of the restriction of motion at nanosecond or faster time scales. Large values of S^2 imply more order (an S^2 of 1 refers to complete restriction). The correlation time τ_o characterizes the tumbling of the molecule with higher values corresponding to a more expanded state. The τ_e characterizes the internal motion of the bond vector.

An alternative approach that we have used as well is the spectral density mapping approach, which has the advantage of not requiring the assumption of isotropic tumbling. The method relies on the simplification of the above expressions by replacing the linear combinations of the values of the spectral density function evaluated at ω_H and $\omega_H \pm \omega_N$ with a single spectral density term.[56] This is a preferred method for analysis of dynamics of denatured states because isotropic tumbling assumption may not be valid. Greater mobility is indicated by lower $J(0)$ and $J(\omega_N)$, and higher $J(\omega_H)$. Nonrandom regions of the protein that are in intermediate exchange are identified by low T_2 and high $J(0)$ values since they contain contributions from motions slower than overall tumbling.

For a rapidly interconverting ensemble of conformations, chemical shifts, NOE intensities, coupling constants, and relaxation parameters are averaged to a single value for the entire ensemble. If the conformations interconvert more slowly on the nmr time scale, nmr parameters give information about separate conformations. While most partially folded proteins report exchange in the fast or intermediate time scale, the partially folded BPTI analogue shows a slow exchange between families of conformations (P_f and P_d), that within themselves are undergoing fast and intermediate conformational exchange. This slow exchange allows for characterization of individual partially folded conformations at equilibrium. In unfolded BPTI variants, different segments of the protein undergo either fast or intermediate exchange. We have characterized the structure in unfolded and partially folded BPTI, in the studies outlined below, at a wide range of time regimes from picosecond to second.

PARTIALLY FOLDED ENSEMBLE

At low temperature and pH $>$ 4.5, $[14–38]_{Abu}$ is an ensemble of partially folded conformations, collectively abbreviated PF. The structural features of PF (Figure 5 Please see page X) were inferred from nmr chemical shifts, hydrogen exchange rates, and local and nonlocal NOEs. Separate peaks in two-dimensional (2D) homonuclear and heteronuclear spectra were assigned to two (and in one case, three) conformations in slow exchange; for each NH there is a cross peak for a less ordered conformation P_d and a cross peak for a more folded conformation P_f. Within P_f and P_d are multiple conformers that are similar in energy, and all of which are possible folding intermediates (Figure 2). It is our working hypothesis that modification of the native state does not alter the characteristics of P_f, so that the partially folded conformations that we observe are representative of short-lived intermediates populated during folding to the native protein.

For each NH, PF consists of all P_f and P_d conformations.

$$PF = P_f + P_d \qquad \text{(I)}$$

P_f and P_d are in equilibrium,

$$P_f \rightleftharpoons P_d \qquad \text{(II)}$$

with interconversion rate constants on the millisecond or longer time scale. The P_f conformation, like the P_d conformation, is itself an ensemble of conformers with interconversion rates $>$ ms. PF undergoes global unfolding to a denatured state, D. The interactions

Table II Relative Populations[a] of Partially Folded Conformations of $[^{14-18}]_{Abu}$ at 5°C

Residue	% P_f Native-Like	% P_f Non-Native	% P_d Ordered	% P_d Disordered
4, 6		40		60
22, 29, 33	75–95		5–25	
12		40	60	
37	20		60	20
40, 45, 48	25–40			60–75
25	60		40	
27	90		10	
28	40			60
56		20		80

[a] Percentages are approximate relative volumes of exchange cross peaks.

within P_d and D are representatives of folding initiation events.

$$PF \rightleftharpoons D \qquad \text{(III)}$$

Structure of Component Conformations

To determine the ordered structure of $[14–38]_{Abu}$, assignments of chemical shifts, long-, medium-, and short-range NOEs, and hydrogen isotope exchange rates were obtained. Figure 5 shows a model of the structure of the ensemble of conformations, the majority of which have the 18–24 and 29–35 antiparallel β-sheet native-like (blue). The small β-bridge, β-turns, and first turn of the C-terminal helix fluctuate between native-like and non-native-like conformations (light blue). In the rest of the molecule, residues sample multiple non-native conformations (dotted lines). Residues of the antiparallel β-sheet are the slowest to undergo hydrogen isotope exchange, further verifying that the core is less accessible to solvent than the rest of the molecule. Hydrogen isotope exchange reports the exchange of NH to ND, while chemical exchange reports the exchange of the same NH between two conformations.

NOE analysis indicates that the main tertiary interactions involve hydrophobic contacts with the rings of Tyr 21, Tyr 23, and Tyr 35. Hence the structure is stabilized by hydrophobic interactions in the core that are both local (side chains of Tyr 23 to Ala 25) and nonlocal (side chains of Tyr 21 to Ala 48, and Tyr 35 to Ile 18).[26] The loss of structure upon removal of Tyr 21 or Tyr 23 corroborates the idea that hydrophobic interactions in the core are the determinants of stability.[57] Consistent with this idea, replacement of the four cysteines with alanine instead of Abu to give $[14–38]_{Ala}$ also results in the loss of the partially folded structure.[58] Abu has an ethyl side chain that is more hydrophobic than the methyl group in Ala.

We conclude that partially folded BPTI analogue is an ensemble of conformations that have a relatively stable core. The stable structure is not in the vicinity of the 14–38 disulfide bond but rather is in the hydrophobic slow exchange core. The role of the disulfide bond is to lower the entropy of the denatured state, thereby shifting the equilibrium toward a partially folded ensemble with more ordered structure in the core. This idea will be revisited in the description of the unfolded state below.

Relative Populations and Segmental Motions

To characterize the conformations that interconvert slowly on the nmr time scale, we use heteronuclear nmr on selectively ^{15}N-labeled protein. Fifteen strategically placed ^{15}N-labeled residues provide microscopic probes of relative populations of the more folded P_f, and the more disordered P_d, interconverting conformations. Table II lists the percentage of populations in P_f and P_d, and whether they are in a native or non native-like conformation. It is important to note that P_f and P_d are assigned based on their relative ordering, where P_f is the more ordered. P_f may be either native or non-native, as shown in Table II. Residues in the core (22, 29, and 33) report 75–95% native-like and 5–25% disordered conformation, while those in the β-bridge and first turn of the helix (45 and 48) report 25–40% native-like conformations and the rest disordered. For residues 4 and 6, which in native BPTI are in the N-terminal helix, both P_f (40%) and P_d (60%) conformations are disordered.

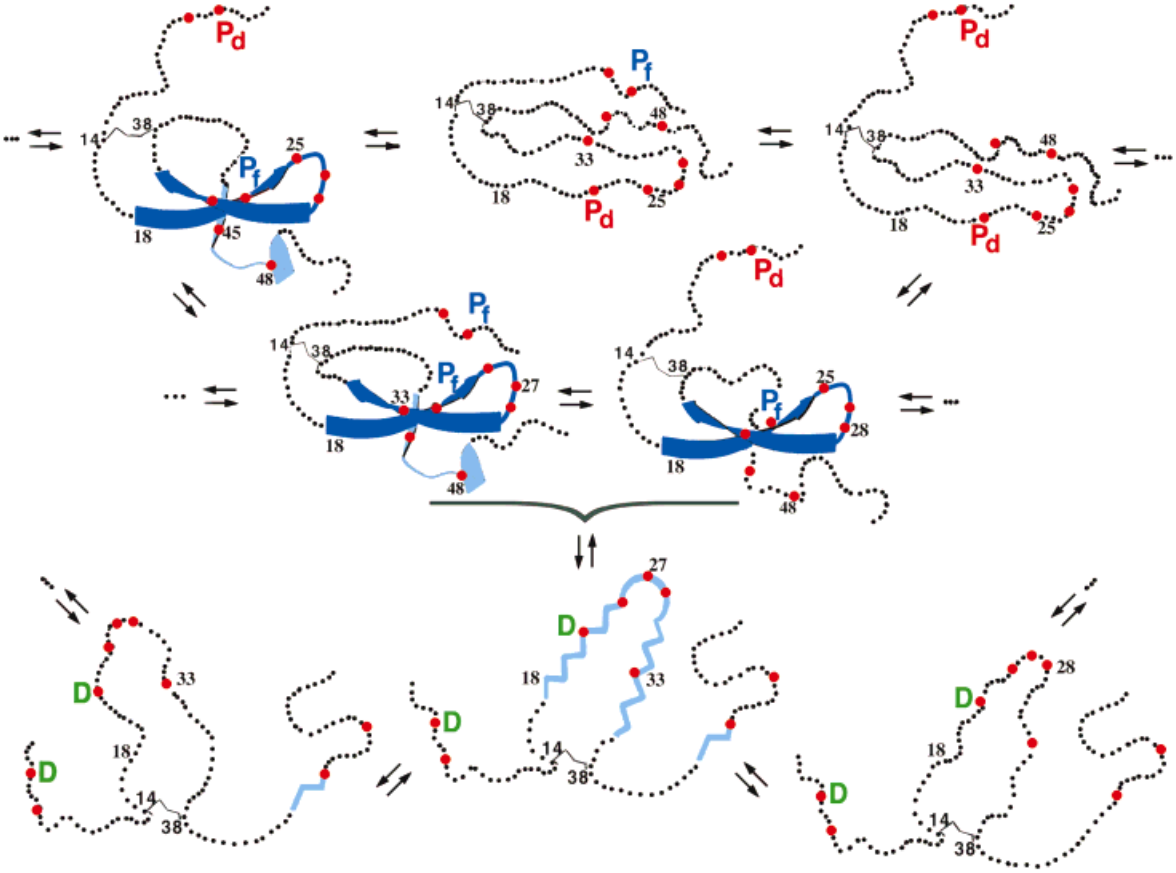

FIGURE 6

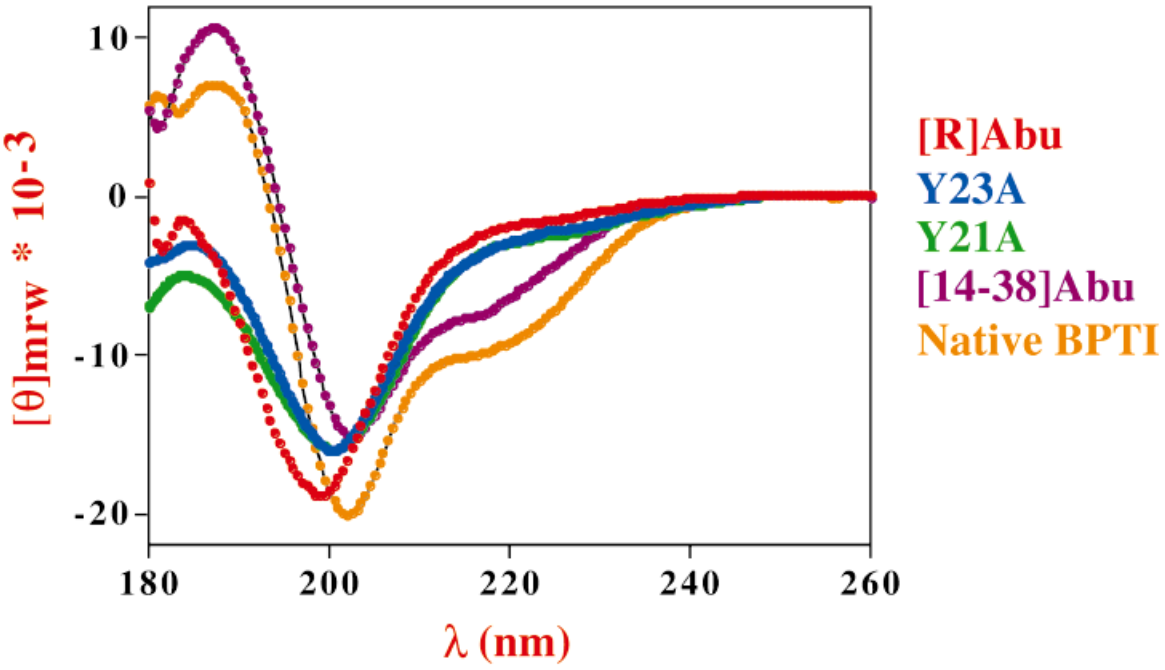

FIGURE 8 Far-uv CD spectra of BPTI variants.

The three turn residues vary in the percentage of P_f and P_d conformations at low temperature. The major conformation for Ala 25 and Ala 27 is P_f, while Gly 28 is P_d, implying that the turn is flexible. For residues in the flexible loops (12, 16, and 40), the major conformation is P_d. There are three observed conformations for 37 with the minor (10%) native-like and the other two are non-native. The Gly 37 NH in native BPTI has a very unusual upfield chemical shift arising from a polar interaction with the center of the Tyr 35 ring.[59]

We conclude that in different parts of the molecule, populations of folded vs disordered conformations vary. Thus, partially folded $[14–38]_{Abu}$ undergoes local fluctuations that are not components of its global cooperative unfolding. A schematic diagram that embodies these ideas is shown in Figure 6.

Interconversion Rates

To obtain interconversion rate constants between P_f and P_d, experiments were carried out at 7°C, the temperature at which segmental local fluctuations are favored. The selectively labeled samples give uncrowded spectra and allow quantitative extraction of intensities from well-resolved cross peaks and their cross-correlation peaks. Exchange spectra acquired at different mixing times show peaks arising from P_f and P_d and two cross-correlation peaks of lower intensity for the forward reaction, P_f to P_d, and the reverse, P_d to P_f. Rate constants k_1 and k_{-1} are obtained for each residue (data shown elsewhere).[45] Values of k_1 vary about an order of magnitude for different residues and range from 0.045 s to 0.44 s^{-1}. Core residues 22 and 33 have the smallest k_1, consistent with NOE and hydrogen exchange results that indicate a native-like stable core in partially folded $[14–38]_{Abu}$. Values of k_{-1} range from 0.1 to 0.88 s^{-1} and are largest for turn residue 27 and core residue 33. The fast rates observed for 27 and 33 relative to other residues suggest that the turn is a nucleation site for formation of the stable core, and the core residue is part of an additional nucleation site. Different P_f to P_d interconversion rates complements our finding of different P_f and P_d populations.

Several conclusions are apparent from measurements of P_f and P_d interconversion rates. First, there are slow, independent, local fluctuations between P_f and P_d involving different segments with substantial energy barriers. Second, the rate for P_f to P_d varies in different parts of the molecule, and is lowest for core residues. Likewise the rate for P_d to P_f varies, and is highest for a turn and a core residue.

Intermediate and Fast Motions

^{15}N-nmr relaxation measurements have been reported for several partially folded proteins.[60–66] Values of order parameters in nonordered regions range from 0.05 to 0.4 while for ordered segments, they are as high as 0.9. High order parameters are observed for core residues when the core is intact while low numbers suggest that the core is disrupted. Another parameter that was used to indicate presence of structure is line broadening due to intermediate exchange. Partially folded and unfolded proteins have residues that exhibit exchange broadening; these regions are considered to be folding nucleation sites. For partially folded BPTI, we characterize the dynamics at individual residue sites of both conformations P_f and P_d.

Dynamics of P_f. Based on data obtained from parameters shown in Table I, the P_f conformation is more compact and more ordered relative to P_d. Order parameters of P_f are around 0.8–0.9 for the core residues and slightly less for the outer segments. These numbers are similar to order parameters of folded proteins with a rigid core. There are few variations within P_f along the polypeptide chain. The core residues 22, 29, and 33 are more ordered than the others, while the N-terminal and part of the C-terminal segments 4, 6, and 56 are least ordered. No evidence of intermediate motions is detected; instead, all conformers within P_f interconvert rapidly. Higher disorder in P_f of residues 4 and 6 are consistent with the absence of medium- and long- range NOEs. This shows that while P_f of the N-terminal segment is more ordered than P_d, it is less native-like and more mobile than P_f conformations of central β-sheet, turn, β-bridge, and first turn of the C-terminal helix.

FIGURE 6 Schematic representation of the conformational ensembles of $[14–38]_{Abu}$ in the partially folded state, PF, and the unfolded state, D. Red circles show the positions of residues labeled with ^{15}N. For *each* ^{15}N-bound ^{1}H in partially folded $[14–38]_{Abu}$, there are both slow ($\geq$ms) local fluctuations (top) between P_f, a more folded conformation, and P_d, a more disordered conformation. At higher temperature the NH may also be in D, a globally denatured conformation (bottom). The labels P_f, P_d, and D are for residues 4 and 22 in each specific conformation.

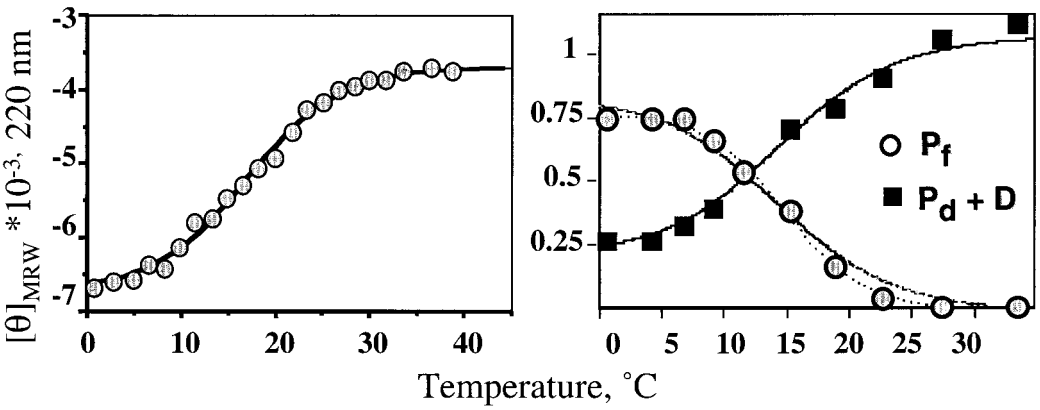

FIGURE 7 Temperature dependence of CD molar ellipticity at 220 nm (left) and nmr cross-peak volumes for residue 22 (right). The "P_f curve" is the variation of (f) cross-peak volumes of Figure 4 with temperature (circles) and the "P_d+ D curve" is the variation of (u) peak volumes with temperature (squares), since there is no difference in chemical shift detected between P_d and D. The dashed line is a fit to individual (f) curves. Solid lines represent the simultaneous fits to all (f) and (u) curves of other residues. The T_m obtained by CD is 19°C and by nmr is 15°C for residue 22.

Dynamics of P_d. The overall correlation time τ_o of 10.1 ns for P_d indicates that it is more expanded relative to P_f (τ_o of 8.4 ns). These results are not surprising in light of our assignment of P_d, as the more disordered conformation. However, new features of P_d emerge from the present results: within P_d there are differences in the dynamics at the various sites along the chain. Motions on the picosecond–nanosecond time scale are greatest for the N-terminal segment, followed by the 45–48 segment, and least for core and turn residues. Order parameters of all NH groups except for those in the core are in the 0.35–0.5 range. This value is similar to order parameters of flexible linkers and loop regions of proteins.[67] Values for core residues are in 0.6–0.7 range, smaller than those in P_f but significantly higher that the rest of P_d. A second indication of differences in dynamics at the various backbone sites is that core residues 22 and 33, and turn residues 25 and 27, undergo intermediate exchange among P_d conformers on the microsecond–millisecond time scale, indicated by diminished T_2 and higher $J(0)$ for these residues, while the other residues are in fast exchange. Intermediate exchange was also verified by a shorter T_2 at higher field (600 vs 500 MHz). Intermediate exchange of core and turn residues in P_d is consistent with observed deviations from random coil NH chemical shifts ($\Delta\delta$); for example, Ala 27 (0.52 ppm), Phe 22 (0.37 ppm), and Phe 33 (0.32 ppm; Figure 4). Intermediate exchange, together with nonrandom chemical shifts and picosecond–nanosecond dynamics, show that P_d conformers of 22, 25, 27, and 33 include more ordered species than P_d conformers of other residues. We conclude that interactions in the core are more stable in P_d as well as in P_f relative to the rest of the molecule.

Characterization of the Transition Between PF and D

So far we have shown that the partially folded ensemble, PF, is a mixture of slowly interconverting conformations P_f and P_d. We have characterized the structure, dynamics of different conformations, their relative population, and interconversion rates at low temperatures (1–7°C). At higher temperature, the partially folded ensemble is destabilized and a denatured ensemble D is populated. Figure 6 shows a schematic presentation of the different conformations populated at 7°C (upper part) and after unfolding at temperatures above 15–19°C (lower part). The model diagram for the denatured ensemble is based on NOEs and chemical shifts of unfolded $[14–38]_{Abu}$. $[14–38]_{Abu}$ is either unfolded at elevated temperature or by point mutations of key residues that cause loss of the partially folded structure.

Stability. The stability of partially folded $[14–38]_{Abu}$ is measured using heteronuclear nmr of selectively labeled species. By measuring the intensity of the NH signal in $^1H–^{15}N$ HSQC spectra at temperatures between 1 and 35°C, we obtain thermal unfolding curves for individual residues in two different conformations. Figure 7 shows representative data for one residue in two conformations P_f and P_d. For residue 22, 75% of the population is in the P_f conformation in exchange with the P_d conformation in the 1–10°C

temperature range. Each residue shows a different preequilibrium before unfolding—for example, residue 6 is 40% P_f. Different populations imply that various segments of the protein vary in the extent to which they are disordered in the partially folded ensemble. We refer to this process as segmental fluctuations.[44] Global unfolding, an equilibrium between the partially folded and denatured ensembles (PF and D), is dominant as the temperature is raised above the transition midpoint. While segmental fluctuation is not cooperative, global thermal unfolding displays features of a cooperative transition, i.e., a similar T_m of 15°C for different residues. The deviation from standard two-state folding/unfolding is indicated by a difference in T_m measured by CD vs nmr, 19°C for CD vs 15°C for nmr, and a small reproducible difference in T_m values between the N-terminal residues and those in the core (17 vs 15°C). The T_m value obtained by CD is not concentration dependent (Barbar, unpublished data), and hence the difference between CD and nmr is not due to aggregation. It is probably because CD is a macroscopic measure of an ensemble averaged signal, while nmr is a microscopic measure of the effect of unfolding at specific sites within the molecule.

Interconversion Rates at Unfolding Conditions. The interconversion rates between P_f and D were measured at 18°C, where the transition to D is favored. At temperatures much above the T_m (>18°C), the intensities of the (f) peaks are completely diminished, not allowing for exchange experiments to be performed. Peak intensities for both (f) and (u) are needed for rate measurement. At 18°C, (f) cross peaks are still measurable and report P_f, and (u) cross peaks primarily report D; k_1 and k_{-1} are rate constants for the transitions of P_f to D and D to P_f, respectively. The rates obtained are similar for different residues, showing that thermal unfolding is more cooperative than segmental fluctuation with a 3-fold variation in rate constants compared to 10-fold. The small difference in folding/unfolding rates, however, is consistent with the lower degree of cooperation and the deviation from two-state unfolding of P_f to D observed for thermal denaturation.

DENATURED ENSEMBLE

The nmr studies of denatured states give insight into the conformations and interactions favored in initial stages of folding, and in early intermediates formed during folding. Similar to partially folded, denatured proteins cannot be thought of as having one or a few conformations.[68] Denatured states consist of numerous interconverting conformations that are unpacked to varying extents, and this critically influences how their structural properties are deciphered by nmr.[37] We have described methods for identification of the segments that are most ordered in partially folded ensembles. In this section we review the nmr characterization of "residual" ordered structure in unfolded BPTI. Analogues of unfolded BPTI are chemically synthesized, reduced BPTI, $[R]_{Abu}$, with all six cysteines replaced by Abu, and two unfolded variants of $[14–38]_{Abu}$—Y21A$[14–38]_{Abu}$ and Y23A$[14–38]_{Abu}$—obtained by chemical synthesis of $[14–38]_{Abu}$ with Tyr 21 or Tyr 23 replaced by alanine. Tyr 21 and Tyr 23 were chosen for mutation because they are involved in important nonlocal and local hydrophobic interactions in partially folded $[14–38]_{Abu}$. All three proteins show almost identical CD spectra (Figure 8 Please see page 200) but their nmr spectra indicate subtle differences. Here again, we demonstrate the utility of nmr in characterizing minor conformations of proteins in which the CD spectra show no stable secondary and tertiary structures. The nmr technique also probes differences in "residual" structure among denatured states. Our results show that the denatured ensemble of BPTI is not a fully random coil but collapsed with some ordered structure.[69,70] There are several interesting differences among the denatured states. Unfolded reduced BPTI with all three disulfide bonds broken sample non-native conformations that are *absent* in the unfolded 14–38 BPTI analogues. Moreover, NOE pattern and exchange broadening differences are observed between the two single disulfide analogues.

Structure

$[R]_{Abu}$, Y21A$[14–38]_{Abu}$, and Y23A$[14–38]_{Abu}$ are unfolded based on their CD spectra (Figure 8) and the loss of chemical shift dispersion in the two-dimensional ^{1}H-nmr spectra (Figures 3 and 9). The presence of ordered structure, however, is inferred from deviations of chemical shifts from the random coil envelope. For example, the Ala 27 and Ala 40 NH chemical shifts show a 0.5 ppm deviation from the random coil region in Y21A$[14–38]_{Abu}$, but are in the random coil region in Y23A$[14–38]_{Abu}$ and reduced BPTI. This upfield chemical shifts shows that there is more ordered structure in one variant relative to the other. Other residues that display dramatic chemical shifts differences are Gly 12 and Gly 37 NH. In reduced BPTI, both Gly residues interact with Tyr rings two residues away resulting in an upfield shifted chemical shifts.[70,71] These interactions are not observed in the

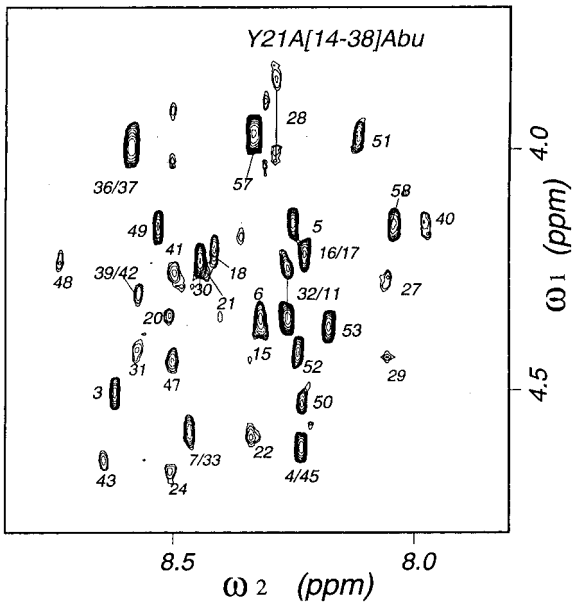

FIGURE 9 1H TOCSY spectrum of Y21A[14–38]$_{Abu}$ with NH-CαH assignments. Diminished intensity in some NH-CαH cross peaks is due to intermediate exchange line broadening on the microsecond–millisecond time scale. Cross peaks in reduced BPTI spectra show similar intensity, indicating fast conformational exchange for residues (data not shown).

other unfolded variants since no upfield shift nor NOEs to Tyr ring are observed. In partially folded [14–38]$_{Abu}$, Gly 37 NH is observed in 3 conformers with different chemical shifts,[26] implying that the interaction with Tyr 35 is strong in two conformers, while the third conformer is disordered. In native BPTI, the 35–37 aromatic–NH interaction shifts Gly 37 NH to around 4 ppm.[59]

Ordered structure was also inferred from sequential and medium-range NOEs. In reduced BPTI, there are strong *non-native* amide–amide NOEs indicating turn-like conformations in one segment that corresponds to an extended β-strand in native BPTI. These NOEs are present to a smaller extent in Y23A[14–38]$_{Abu}$ and are completely missing in Y21A[14–38]$_{Abu}$, where they are replaced by native-like NOEs. In Y23A[14–38]$_{Abu}$ and Y21A[14–38]$_{Abu}$, there are few native-like backbone amide–amide sequential NOEs for segments that correspond to the first turn of the C-terminal helix, the N-terminal helix, and turns in native BPTI. Aromatic–aliphatic NOEs are mostly local and they correspond to core residues in native BPTI. Both native and non-native NOEs are observed in reduced BPTI, but in the variants with a single disulfide, non-native NOEs are replaced with native nonlocal contacts that are mainly hydrophobic. Based on the intensity and number of NOEs, Y21A[14–38]$_{Abu}$ shows the most ordered native-like structure relative to other variants. A model of unfolded BPTI based on the structural data is shown in Figure 10, illustrating that unfolded BPTI is collapsed and that there are structural differences observed in the unfolded state upon introduction of a single disulfide bond.

Chemical Exchange and Dynamics

Intermediate conformational exchange in unfolded [14–38]$_{Abu}$ variants was inferred from peak broadening in homonuclear TOCSY spectra (Figure 9). Intermediate chemical exchange results in a signal that is broadened, while fast or slow chemical exchange gives a single average signal or separate signals for each conformation, respectively. In both unfolded [14–38]$_{Abu}$ variants, there were narrow and broad peaks in the same spectrum. Resonance assignments of all peaks revealed that the ones with the most severe line broadening correspond to residues in the hydrophobic core of native BPTI.[69] In contrast, residues in the N-terminal segment and the first part of the C-terminal helix (48–53) undergo fast chemical exchange, resulting in intense cross peaks in TOCSY and NOESY spectra. These same residues exhibit strong sequential CαH-NH NOEs as well as strong sequential NH-NH NOEs, implying that the ^{1}H signal is averaged over both extended and turn-like conformations. The spectra of reduced BPTI in comparison show uniform line widths for almost all residues.[45] Changes in chemical exchange broadening are consistent with the likelihood that formation of the disulfide bond introduces a small increase in the population of partially folded structures.

The interesting conclusion from chemical exchange broadening is that intermediate exchange is localized in the region that corresponds to the hydrophobic core in native BPTI. More order in the core residues is supported by heteronuclear relaxation measurements performed on unfolded [14–38]$_{Abu}$ at an elevated temperature.[45] While exchange broadening indicates ordered structure on the millisecond–microsecond time scale, dynamics measurements on the nanosecond–picosecond time scale also show a distinct difference in flexibility, with the most order being in the region corresponding to the slow exchange core. A schematic drawing of the ensemble of unfolded BPTI with a single disulfide bond is shown in the bottom part of Figure 6.

Hydrodynamic Measurements

The hydrodynamic behavior of unfolded and partially folded BPTI was examined by pulsed-field gradient

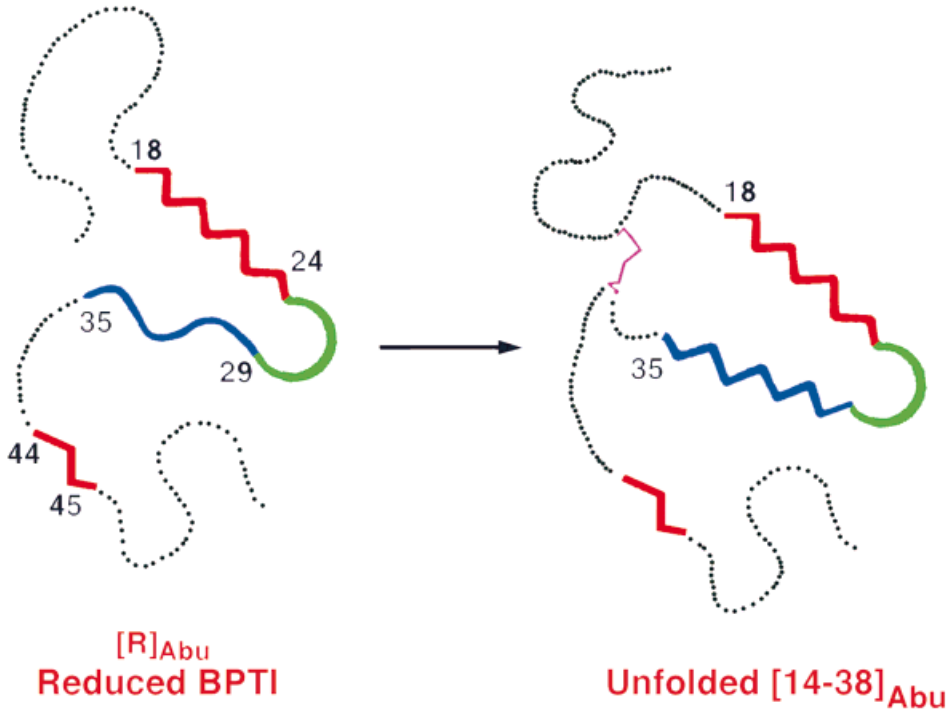

FIGURE 10 A model of unfolded BPTI with a single disulfide compared with reduced BPTI. Both have compact structure with more order in the core. Non-native interactions, shown in blue, in reduced BPTI between residues 29 and 35 are replaced by native-like extended conformations in unfolded $[14–38]_{Abu}$.

nmr experiments that measure the translational diffusion coefficient of a molecule in solution. Pulse-field gradients allow for generation of a gradient across the sample, which can then be used to measure diffusion of the molecule and therefore probe the molecular radius.[72] The hydrodynamic radii of unfolded and partially folded variants show significant expansion when compared to native. The hydrodynamic radius for native BPTI is 15.2 Å, while both reduced BPTI, and unfolded $[14–38]_{Abu}$ have similar hydrodynamic radii of 20.6 and 20.7 Å, respectively.[73] These numbers indicate that unfolded BPTI is more collapsed than random coil (estimated radius of 23.6 Å). Partially folded $[14–38]_{Abu}$ is fairly compact with a radius of hydration of 18.1 Å, expanded by about 19% relative to native.

Denatured States of BPTI Differ in Their Ordered Structure

Denatured BPTI is not a random coil but is collapsed. To summarize our results from nmr studies, the residual structure is inferred from short- and medium-range NOEs, exchange broadening, chemical shift dispersion for few residues, smaller hydrodynamic radii than random coil, and considerable order on the fast nanosecond–picosecond time scale. The important outcomes are 2-fold: First, the compact structure detected in unfolded BPTI corresponds to the slow exchange stable core in native. This demonstrates that there are collapsed species organized in the core segments in the unfolded ensemble, a very interesting conclusion. Second, there is a significant difference in the distribution of conformational substates of unfolded reduced BPTI as compared to unfolded BPTI with the 14–38 disulfide crosslink. The striking, *non-native*, amide–amide and aromatic–aliphatic NOEs of contiguous residues of one segment 29–35 in reduced BPTI are not present in $Y21A[14–38]_{Abu}$ and $Y23A[14–38]_{Abu}$. In addition, specific differences between $Y21A[14–38]_{Abu}$ and $Y23A[14–38]_{Abu}$ indicate that replacement of Tyr 23 results in less ordered structure than replacement of Tyr 21. These

differences are consistent with multiple folding pathways of different denatured states present at the starting points of folding.

CONCLUSION

We have obtained perhaps the most complete ensemble description of partially folded and unfolded proteins. We take these as models for transiently populated intermediates during early folding events. The chemically synthesized variants offer an experimental system for characterization of the interconverting conformations populated in initial stages of folding. The slowly interconverting multiple conformations allow characterization of new ensemble parameters, including the number and structure of compact conformations, their dynamics, relative population, and interconversion rates. The most ordered, native-like region is in the secondary structural elements that make up the slow exchange core. Similarly, unfolded states are also ensembles of conformations. There is considerable nonrandom structure in unfolded BPTI, the structure is compact and displays significant differences among denatured states.

The role of the disulfide bonds in BPTI folding has been the subject of several controversies and reviews.[74,75] Our results suggest that when any one of the native disulfide bonds is formed, the core is stabilized while the rest of the molecule is more flexible. Stabilization of the core is primarily a chain entropy effect on the denatured states, where stable unfolded conformations are eliminated from the distribution and the more favored collapsed conformations are formed. When 14–38 is the only cross-link, ordered structure is formed *not* in the vicinity of the disulfide but in the slow exchange core distant from the disulfide. Further, the order of disulfide bond formation is *not* a critical factor in folding. Any single disulfide bond leads to native-like structure in the core. The role of the second and third disulfide bonds is to eliminate flexible conformations of segments outside the core. In the unfolded ensemble, the 14–38 disulfide destabilizes non-native conformations and thereby shifts the conformational ensemble towards partially folded structures.

In all partially folded and unfolded states, the ordered structure is in the most stable core. This is consistent with the hypothesis that the residues that are the first to fold go on to form the most stable, structure-determining part of the protein.[76] The ensemble nature of both partially folded and unfolded states supports the idea of multiple folding routes instead of a single trajectory. At different stages during folding, there is an ensemble of nondiscrete conformations that are native-like and productive in their path to the native.

The author thanks Professors Clare Woodward and George Barany at the University of Minnesota for excellent collaboration and support. This work was supported by NIH grants GM 26242 (CW), GM 51628 (GB and CW), and GM 17341 (EB).

REFERENCES

1. Brooks, C. L.; Gruebele, M.; Onuchic, J. N.; Wolynes, P. G. Proc Natl Acad Sci USA 1998, 95, 11037–11038.
2. Chan, H. S.; Dill, K. A. Proteins Struct Funct Genet 1998, 30, 2–33.
3. Dill, K. A.; Chan, H. S. Nature Struct Biol 1997, 4, 10–19.
4. Socci, N. D.; Onuchic, J. N.; Wolynes, P. G. Proteins Struct Funct Genet 1998, 32, 136–158.
5. Onuchic, J. N.; Socci, N. D.; LutheySchulten, Z.; Wolynes, P. G. Folding Design 1996, 1, 441–450.
6. Thirumalai, D.; Woodson, S. A. Acc Chem Res 1996, 29, 433–439.
7. Onuchic, J. N.; LutheySchulten, Z.; Wolynes, P. G. Ann Rev Phys Chem 1997, 48, 545–600.
8. Dobson, C. M.; Sali, A.; Karplus, M. Angew Chem Intl Ed Eng 1998, 37, 868–893.
9. Pande, V. S.; Grosberg, A. Y.; Tanaka, T.; Rokhsar, D. S. Curr Opin Struct Biol 1998, 8, 68–79.
10. Anfinson, C. B. Science 1973, 181, 223–230.
11. Horwich, A. L.; Weissman, J. S. Cell 1997, 89, 499–510.
12. Lansbury, P. T. Curr Opin Chem Biol 1997, 1, 260–267.
13. Conway, K. A.; Harper, J. D.; Lansbury, P. T. Nature Med 1998, 4, 1318–1320.
14. Guijarro, J. I.; Sunde, M.; Jones, J. A.; Campbell, I. D.; Dobson, C. M. Proc Natl Acad Sci USA 1998, 95, 4224.
15. Chiti, F.; Webster, P.; Taddei, N.; Clarek, A.; Stefani, M.; Ramponi, G.; Dobson, C. M. Proc Natl Acad Sci USA 1999, 96, 3590–3594.
16. Jennings, P.; Wright, P. Science 1993, 262, 892–896.
17. Balbach, J.; Forge, V.; van Nuland, N. A.; Winder, S. L.; Hore, P. J.; Dobson, C. M. Nature Struct Biol 1995, 2, 865–870.
18. Alexandrescu, A. T.; Evans, P. A.; Pitkeathly, M.; Baum, J.; Dobson, C. M. Biochemistry 1993, 32, 1707–1718.
19. Buck, M.; Radford, S. E.; Dobson, C. M. Biochemistry 1993, 32, 669–678.
20. Falzone, C. J.; Mayer, M. R.; Whiteman, E. L.; Moore, C. D.; Lecomte, J. T. Biochemistry 1996, 35, 6519–6526.
21. Molinari, H.; Ragona, L.; Varani, L.; Musco, G.; Consonni, R.; Zetta, L.; Monaco, H. L. FEBS Lett 1996, 381, 237–243.

22. Ewbank, J. J.; Creighton, T. E. Biochemistry 1993, 32, 3694–3707.
23. Shimotakahara, S.; Rios, C. B.; Laity, J. H.; Zimmerman, D. E.; Scheraga, H. A.; Montelione, G. T. Biochemistry 1997, 36, 6915–6929.
24. Staley, J. P.; Kim, P. S. Protein Sci 1994, 3, 1822–1832.
25. van, M. C.; Kemmink, J.; Neuhaus, D.; Darby, N. J.; Creighton, T. E. J Mol Biol 1994, 235, 1044–1061.
26. Barbar, E.; Barany, G.; Woodward, C. Biochemistry 1995, 34, 11423–11434.
27. Ferrer, M.; Barany, G.; Woodward, C. Nature Struct Biol 1995, 2, 211–218.
28. Alexandrescu, A. T.; Abeygunawardana, C.; Shortle, D. Biochemistry 1994, 33, 1063–1072.
29. Reymond, M. T.; Merutka, G.; Dyson, H. J.; Wright, P. E. Protein Sci 1997, 6, 706–716.
30. Dyson, H. J.; Wright, P. E. Curr Opin Struct Biol 1993, 3, 60–65.
31. Blanco, F. J.; Rivas, G.; Serrano, L. Nature Struct Biol 1994, 1, 584–590.
32. Bryson, J. W.; Betz, S. F.; Lu, H. S.; Suich, D. J.; Zhou, H. X. X.; Oneil, K. T.; Degrado, W. F. Science 1995, 270, 935–941.
33. Ramirez-Alvarado, M.; Kortemme, T.; Blanco, F. J.; Serrano, L. Bioorg Med Chem 1999, 7, 93–103.
34. Kemmink, J.; Creighton, T. E. Biochemistry 1995, 34, 12630–12635.
35. Dyson, H. J.; Wright, P. E. Ann Rev Phys Chem 1996, 47, 369–395.
36. Dyson, H. J.; Wright, P. E. Nature Struct Biol 1998, 5, 499–503.
37. Shortle, D. R. Curr Opin Struct Biol 1996, 6, 24–30.
38. Schulman, B. A.; Kim, P. S.; Dobson, C. M.; Redfield, C. Nature Struct Biol 1997, 4, 630–634.
39. Wang, Y.; Shortle, D. Biochemistry 1995, 34, 15895–15905.
40. Eliezer, D.; Yao, J.; Dyson, H. J.; Wright, P. E. Nature Struct Biol 1998, 5, 148–155.
41. Buck, M.; Schwalbe, H.; Dobson, C. M. Biochemistry 1995, 34, 13219–13232.
42. Fong, S.; Bycroft, M.; Clarke, J.; Freund, S. M. V. J Mol Biol 1998, 278, 417–429.
43. Schonbrunner, N.; Wey, J.; Engels, J.; Georg, H.; Kiefhaber, T. J Mol Biol 1996, 260, 432–445.
44. Barbar, E.; LiCata, V.; Barany, G.; Woodward, C. Biophys Chem 1997, 64, 45–57.
45. Barbar, E.; Hare, M.; Daragan, V.; Barany, G.; Woodward, G. Biochemistry 1998, 37, 7822–7833.
46. Barbar, E.; Gross, C. M.; Woodward, G.; Barany, G. Methods Enzymol 1997, 289, 587–611.
47. Staley, J. P.; Kim, P. S. Proc Natl Acad Sci USA 1992, 89, 1519–1523.
48. van, M. C.; Darby, N. J.; Neuhaus, D.; Creighton, T. E. J Mol Biol 1991, 222, 373–390.
49. van, M. C.; Darby, N. J.; Keeler, J.; Neuhaus, D.; Creighton, T. E. J Mol Biol 1993, 229, 1125–1146.
50. Wishart, D. S.; Sykes, B. D.; Richards, F. M. J Mol Biol 1991, 222, 311–333.
51. Sandström, J. Dynamic NMR; Academic Press: New York, 1982.
52. Bax, A.; Davis, D. G. J Magn Reson 1985, 63, 207–213.
53. Peng, J. W.; Wagner, G. Methods Enzymol 1994, 239, 563–596.
54. Kay, L. E. Biochem Cell Biol 1997, 75, 1–15.
55. Daragan, V. A.; Mayo, K. H. Progr NMR Spectrosc 1997, 31, 63–105.
56. Farrow, N. A.; Zhang, O. W.; Szabo, A.; Torchia, D. A.; Kay, L. E. J Biomol NMR 1995, 6, 153–162.
57. Kim, K. S.; Fuchs, J. A.; Woodward, C. K. Biochemistry 1993, 32, 9600–9608.
58. Dadlez, M.; Kim, P. S. Nature Struct Biol 1995, 2, 674–679.
59. Tüchsen, E.; Woodward, C. Biochemistry 1987, 26, 1918–1925.
60. Buck, M.; Schwalbe, H.; Dobson, C. M. J Mol Biol 1996, 257, 669–683.
61. Lefevre, J. F.; Dayie, K. T.; Peng, J. W.; Wagner, G. Biochemistry 1996, 35, 2674–2686.
62. Frank, M. K.; Clore, G. M.; Gronenborn, A. M. Protein Sci 1995, 4, 2605–2615.
63. Bhattacharya, S.; Falzone, C. J.; Lecomte, J. T. J. Biochemistry 1999, 38, 2577–2589.
64. Brutscher, B.; Bruschweiler, R.; Ernst, R. R. Biochemistry 1997, 36, 13043–13053.
65. Alexandrescu, A. T.; Shortle, D. J Mol Biol 1994, 242, 527–546.
66. Redfield, C.; Smith, R. A.; Dobson, C. M. Nature Struct Biol 1994, 1, 23–29.
67. Akke, M.; Forsen, S.; Chazin, W. J. Magn Reson Chem 1993, 31, S128–S132.
68. Dill, K. A.; Shortle, D. Ann Rev Biochem 1991, 60, 795–825.
69. Barbar, E.; Barany, G.; Woodward, C. Folding Design 1996, 1, 65–76.
70. Pan, H.; Barbar, E.; Barany, G.; Woodward, C. Biochemistry 1995, 34, 13974–13981.
71. Kemmink, J.; Creighton, T. E. J Mol Biol 1993, 234, 861–788.
72. Altieri, A. S.; Hinton, D. P.; Byrd, R. A. J Am Chem Soc 1995, 117, 7566–7567.
73. Pan, H.; Barany, G.; Woodward, G. Protein Sci 1997, 6, 1985–1992.
74. Creighton, T. E. Bioessays 1992, *14*, 195–199.
75. Darby, N. J.; Morin, P. E.; Talbo, G.; Creighton, T. E. J Mol Biol 1995, 249, 463–477.
76. Woodward, C.; Li, R. H. Trends Biochem Sci 1998, 23, 379–379.